Osmosensory signaling in *Mycobacterium tuberculosis* mediated by a eukaryotic-like Ser/Thr protein kinase

Stavroula K. Hatzios[a], Christina E. Baer[b], Tige R. Rustad[c,d], M. Sloan Siegrist[a], Jennifer M. Pang[c,d], Corrie Ortega[c,d], Tom Alber[b], Christoph Grundner[c,d], David R. Sherman[c,d], and Carolyn R. Bertozzi[a,b,e,1]

Departments of [a]Chemistry and [b]Molecular and Cell Biology, California Institute for Quantitative Biosciences (QB3), and [e]Howard Hughes Medical Institute, University of California, Berkeley, CA 94720; [c]Seattle Biomedical Research Institute, Seattle, WA 98109; and [d]Department of Global Health, University of Washington, Seattle, WA 98195

Contributed by Carolyn R. Bertozzi, November 11, 2013 (sent for review July 17, 2013)

Bacteria are able to adapt to dramatically different microenvironments, but in many organisms, the signaling pathways, transcriptional programs, and downstream physiological changes involved in adaptation are not well-understood. Here, we discovered that osmotic stress stimulates a signaling network in *Mycobacterium tuberculosis* regulated by the eukaryotic-like receptor Ser/Thr protein kinase PknD. Expression of the PknD substrate Rv0516c was highly induced by osmotic stress. Furthermore, *Rv0516c* disruption modified peptidoglycan thickness, enhanced antibiotic resistance, and activated genes in the regulon of the alternative σ-factor SigF. Phosphorylation of Rv0516c regulated the abundance of EspA, a virulence-associated substrate of the type VII ESX-1 secretion system. These findings identify an osmosensory pathway orchestrated by PknD, Rv0516c, and SigF that enables adaptation to osmotic stress through cell wall remodeling and virulence factor production. Given the widespread occurrence of eukaryotic-like Ser/Thr protein kinases in bacteria, these proteins may play a broad role in bacterial osmosensing.

environmental sensing | extracellular osmolarity | transcriptional regulation | type VII secretion

Bacteria are notoriously adaptive to conditions of environmental stress and antibiotic challenge (1, 2). The bacterial response to extracellular signals relies on diverse transcriptional regulators. The best characterized of these regulators are two-component systems (TCSs) and alternative σ-factors (3–6). Although TCSs are widely distributed among prokaryotes and eukaryotes, alternative σ-factors are found only in bacteria (3, 5).

TCSs consist of a membrane-associated sensor histidine kinase and a cognate response regulator, which typically alters gene expression following its phosphorylation by the sensor kinase (3). Alternative σ-factors (also known as extracytoplasmic function σ-factors) regulate transcription by binding RNA polymerase and recruiting it to specific promoters (5). This activity is tightly controlled by anti–σ-factors, which bind cognate σ-factors and prevent their association with RNA polymerase (7, 8). A third group of proteins, the anti-anti–σ-factors, facilitate dissociation of this inhibitory complex by binding the anti–σ-factor (9). In turn, some anti–σ-factors have been shown to phosphorylate the anti-anti–σ-factor on a conserved serine or threonine residue, liberating the anti–σ-factor for another round of protein–protein interactions (10, 11). This phosphorylation is reversed by an environmental phosphatase, which is itself regulated by a separate set of anti–σ- and anti-anti–σ-factor homologs (11).

Less well-understood are the receptor Ser/Thr protein kinases (STPKs). These receptor kinases are important mediators of environmental sensing in eukaryotes (12–14). Genome sequencing has revealed that eukaryotic-like STPKs are widespread in bacteria, but with few exceptions, the specific biological functions of these kinases are undefined (15). As in eukaryotes, they may play a critical role in environmental sensing and downstream signaling.

Eukaryotic-like STPKs have been most extensively studied in *Mycobacterium tuberculosis* (*Mtb*), the bacterial pathogen that causes tuberculosis (16–18). Of 11 *Mtb* STPKs, the best described is PknB, which is believed to regulate cell wall biosynthesis and cell division (19–21). The extracellular domain of PknB binds peptidoglycan (PG)-derived muropeptides (22), and the kinase exerts downstream effects on cell wall synthesis, cell shape, cell division, transcription, and translation (20, 23, 24). Similarly, the homologous *Bacillus subtilis* STPK PrkC has been shown to bind muropeptides that induce the germination of dormant spores, most likely by stimulating the PrkC-dependent phosphorylation of a ribosomal GTPase (25–27). Beyond this example, however, the precise environmental signals that trigger STPK signaling in bacteria are unknown, and the downstream processes regulated by these kinases are poorly defined.

Here, we discovered that osmotic stress stimulates a signaling pathway in *Mtb* regulated by the receptor STPK PknD. Our focus on osmotic stress was motivated by the fact that *Mtb* adapts to changes in environmental osmolarity as it transitions between airborne droplet nuclei, mucosal epithelia, alveolar macrophages, necrotic cells, and caseous granulomas (28). Osmotic fluctuations alter turgor pressure, which can impair protein folding and metabolic activity (29). Bacteria typically counteract such fluctuations through the compensatory accumulation or expulsion of compatible solutes that restore osmotic balance to the cell (30). In addition, several bacterial pathogens have virulence-associated osmosensory mechanisms that are triggered at the transcriptional level, typically through TCSs (29, 31–33). We sought to determine whether *Mtb* mounts an analogous response that might lead to physiological adaptations relevant to pathogenesis.

Significance

Osmotic stress is one of many environmental hazards encountered by bacteria during the course of infection, but our understanding of how bacteria perceive and respond to changes in extracellular osmolarity is still incomplete. We show that *Mycobacterium tuberculosis*, the pathogen that causes tuberculosis in humans, responds, in part, through an osmosensory pathway regulated by the Ser/Thr protein kinase (STPK) PknD. Our work demonstrates that increasing extracellular osmolarity induces expression of a PknD substrate that regulates bacterial transcription, cell wall remodeling, and virulence factor production. Because STPKs are prevalent in bacteria, these proteins may play a broad role in bacterial osmosensing.

Author contributions: S.K.H., C.E.B., T.R.R., J.M.P., C.O., T.A., C.G., D.R.S., and C.R.B. designed research; S.K.H., C.E.B., M.S.S., J.M.P., and C.O. performed research; T.R.R. and D.R.S. contributed new reagents/analytic tools; S.K.H., C.E.B., T.R.R., M.S.S., J.M.P., C.O., C.G., D.R.S., and C.R.B. analyzed data; and S.K.H., M.S.S., and C.R.B. wrote the paper.

The authors declare no conflict of interest.

Data deposition: The microarray data reported in this paper have been deposited in the Gene Expression Omnibus (GEO) database, www.ncbi.nlm.nih.gov/geo (accession nos. GSE50159 and GSE50160).

[1]To whom correspondence should be addressed. E-mail: crb@berkeley.edu.

This article contains supporting information online at www.pnas.org/lookup/suppl/doi:10.1073/pnas.1321205110/-/DCSupplemental.

By transcriptional profiling, we found that a PknD substrate, Rv0516c (34), is highly up-regulated by osmotic stress. Disruption of *Rv0516c*, which encodes an anti-anti–σ-factor homolog, modified PG thickness, enhanced antibiotic resistance, and activated genes in the SigF regulon. Furthermore, phosphorylation of Rv0516c by PknD was required to sustain WT levels of the secreted virulence factor EspA, a substrate of the ESX-1 secretion system. We conclude that PknD, Rv0516c, and SigF constitute an osmosensory signaling pathway that regulates PG architecture and EspA abundance. This signaling pathway is a direct demonstration of a transcriptional response to environmental stress mediated by a bacterial STPK. The regulation of SigF activity by PknD after an increase in extracellular osmolarity defines a transcriptional circuit in which environmental sensing by a eukaryotic-like receptor converges with a fundamentally prokaryotic transcriptional regulatory system.

Results

Osmotic Stress Elicits a Significant Transcriptional Response from *Mtb*. To identify mediators of the *Mtb* osmotic stress response, we determined the global transcriptional profile of *Mtb* after an increase in extracellular osmolarity of ∼280 mOsm/L, which is comparable with the osmolarity of human plasma (35). We reasoned that *Mtb* might encounter a similar increase in extracellular osmolarity during the course of infection. Bacteria were grown in a chemically defined culture medium (details in *SI Materials and Methods*) and treated with 140 mM NaCl (∼280 mOsm/L) for 1 h to determine changes in bacterial transcription relative to an untreated control (National Center for Biotechnology Information/Gene Expression Omnibus accession no. GSE50159).

Over 100 induced genes were identified in our microarray analysis (Table 1), many from the same operons. Notably, the entire *arg* operon, which is required for the de novo biosynthesis of L-arginine (37), was induced by osmotic stress. Arginine has been associated with hyperosmotic stress tolerance in yeast (38), suggesting that it may play an osmoprotective role in *Mtb*. The *Rv3616c-Rv3614c* operon, which encodes components of the virulence-associated ESX-1 secretion system (39–41), was also up-regulated, along with several genes involved in sulfur metabolism (e.g., *cysA3*, *csd*, and *sirA*) and ribosomal assembly (e.g., genes from the *rps* and *rpl* operons). These findings imply that increasing osmolarity can activate a unique transcriptional program in *Mtb* that may influence bacterial virulence and facilitate survival during infection. Of note, a subset of induced genes from

Table 1. Genes up-regulated in *Mtb* strain CDC1551 on exposure to 140 mM NaCl

Gene number	Fold change	Gene name	Gene number	Fold change	Gene name	Gene number	Fold change	Gene name
Rv0009	2.1	*ppiA*	Rv0950c	2.7		Rv2890c	2.9	*rpsB*
Rv0055	2.2	*rpsR1*	Rv0952	2.1	*sucD*	Rv3028c	2.4	*fixB*
Rv0056	2.1	*rplI*	Rv1072	2.1		Rv3029c	2.1	*fixA*
Rv0211	2.1	*pckA*	Rv1078	4.0	*pra*	Rv3117	3.5	*cysA3*
Rv0227c	2.3		Rv1297	2.4	*rho*	Rv3118	5.3	*sseC1*
Rv0263c	2.8		Rv1462	2.6		Rv3130c	2.1	*tgs1*
Rv0350	2.1	*dnaK*	Rv1463	3.1		Rv3131	2.5	
Rv0352	2.1	*dnaJ1*	Rv1464	3.3	*csd*	Rv3219	3.3	*whiB1*
Rv0440	2.3	*groEL2*	Rv1466	2.7		Rv3418c	2.7	*groES*
Rv0475	2.3	*hbhA*	Rv1641	2.8	*infC*	Rv3442c	3.2	*rpsI*
Rv0479c	2.4		Rv1642	2.9	*rpmI*	Rv3443c	2.3	*rplM*
Rv0516c	21.2		Rv1643	2.6	*rplT*	Rv3457c	2.4	*rpoA*
Rv0652	3.1	*rplL*	Rv1652	2.5	*argC*	Rv3458c	3.0	*rpsD*
Rv0667	2.9	*rpoB*	Rv1653	7.0	*argJ*	Rv3459c	2.7	*rpsK*
Rv0676c	2.0	*mmpL5*	Rv1654	5.1	*argB*	Rv3460c	2.8	*rpsM*
Rv0682	3.6	*rpsL*	Rv1655	4.9	*argD*	Rv3613c	4.3	
Rv0683	3.8	*rpsG*	Rv1656	2.1	*argF*	Rv3614c	3.9	*espD*
Rv0684	3.0	*fusA1*	Rv1657	2.2	*argR*	Rv3615c	6.5	*espC*
Rv0700	3.1	*rpsJ*	Rv1658	3.0	*argG*	Rv3616c	3.6	*espA*
Rv0701	3.7	*rplC*	Rv1659	2.3	*argH*	Rv3763	2.1	*lpqH*
Rv0702	2.3	*rplD*	Rv1886c	2.6	*fbpB*	Rv3810	2.4	*pirG*
Rv0703	3.6	*rplW*	Rv1908c	2.4	*katG*	Rv3924c	2.5	*rpmH*
Rv0704	3.0	*rplB*	Rv1980c	2.3	*mpt64*	MT0066.1	4.0	
Rv0706	2.4	*rplV*	Rv1996	2.1		MT0066.2	4.8	
Rv0707	2.0	*rpsC*	Rv2050	3.0		MT0835	2.7	
Rv0708	2.4	*rplP*	Rv2190c	2.4		MT1178	11.0	
Rv0709	2.3	*rpmC*	Rv2271	2.7		MT1448	2.9	
Rv0714	2.1	*rplN*	Rv2301	2.6	*cut2*	MT2245	2.6	
Rv0716	2.2	*rplE*	Rv2348c	3.8		MT2420	2.9	
Rv0717	3.0	*rpsN1*	Rv2391	2.4	*sirA*	MT2421	3.3	
Rv0718	3.0	*rpsH*	Rv2412	2.9	*rpsT*	MT2422	3.4	
Rv0719	2.1	*rplF*	Rv2441c	2.7	*rpmA*	MT2460	2.6	
Rv0721	2.0	*rpsE*	Rv2442c	3.0	*rplU*	MT2516	2.3	*obg*
Rv0747	2.9	*PE_PGRS10*	Rv2745c	2.1		MT3217	2.6	
Rv0761c	2.2	*adhB*	Rv2783c	2.2	*gpsI*	MT3562	2.2	*truA*
Rv0867c	2.4	*rpfA*	Rv2889c	2.1	*tsf*	MT3693	2.3	

DNA microarray analysis was used to identify *Mtb* genes significantly induced after 1-h exposure to 140 mM NaCl. Arrays from four biological replicates were analyzed using the Significance Analysis of Microarrays (SAM) program (36). Genes having a mean $\log_2$ fold change of one or greater with an SAM-assigned false discovery rate value (i.e., q value) of <0.06% were deemed significant. Gene names were obtained from TubercuList (http://tuberculist.epfl.ch/) and the J. Craig Venter Institute Comprehensive Microbial Resource (http://cmr.jcvi.org/cgi-bin/CMR/CmrHomePage.cgi).

our analysis was also up-regulated after treatment with 250 mM NaCl for 4 h in a recent microarray study by Tan et al. (42).

Osmotic Stress Induces Rv0516c Expression. The most highly induced gene in our microarray analysis, *Rv0516c*, encodes a hypothetical protein of previously unknown function. To determine whether the enhanced transcription of *Rv0516c* under osmotic stress correlates with an increase in protein expression, we designed a construct encoding Rv0516c with a C-terminal 3xDDDDK tag (*Rv0516c::Tn* + p*Rv0516c*). We placed this construct under direct control of the native *Rv0516c* promoter by deleting the Hsp60 promoter of plasmid pMV261 and inserting the 1,000-bp region immediately upstream of the *Rv0516c* gene. Immunoblotting revealed a sharp increase in Rv0516c expression after the addition of 140 mM NaCl (Fig. 1*A*). Similar expression levels resulted from treatment with two other osmolytes, KCl and sucrose, at concentrations corresponding to an equivalent increase in culture osmolarity (i.e., ~280 mOsm/L). These findings confirm that osmotic stress induces Rv0516c expression in *Mtb*.

We subsequently asked whether the *Rv0516c* promoter could enhance the expression of a reporter gene in response to increasing osmolarity. We quantified the fluorescence of *Mtb* expressing the *gfp* gene under control of the *Rv0516c* promoter after the addition of NaCl, KCl, or sucrose at equal osmolarity. In all cases, osmolyte addition increased GFP fluorescence by roughly the same amount relative to the untreated control (Fig. 1*B*). Overall, these findings suggest that the *Rv0516c* promoter contains an osmotically sensitive regulatory region.

***Rv0516c* Disruption Enhances Resistance to Osmotic Stress.** Given the strong induction of *Rv0516c* by osmotic stress, we reasoned that the encoded gene product might influence the physiological response of *Mtb* to increasing osmolarity. To explore this possibility, we compared the growth kinetics of an *Rv0516c* mutant (*Rv0516c::Tn*) with WT and complemented strains of *Mtb* after hyperosmotic shock with 0.5 M NaCl. Surprisingly, we discovered that *Rv0516c::Tn* was more resistant to increasing osmolarity than WT *Mtb*. The growth kinetics of the mutant strain were unaffected by NaCl treatment, whereas the WT strain exhibited an apparent decline in bacterial replication (Fig. 2 *A* and *B*). Complementation of the mutant strain with a plasmid expressing *Rv0516c* under its native promoter restored WT growth kinetics in the presence of 0.5 M NaCl. However, we were unable to distinguish whether the apparent growth attenuation of the WT and complemented strains was the result of reduced bacterial replication or bacterial clumping, because both strains tended to aggregate after NaCl addition (Fig. 2*C*). In contrast, the mutant strain remained relatively well-suspended in the culture medium, suggesting a change in cell wall structure. *Rv0516c::Tn* also exhibited enhanced growth kinetics in the absence of NaCl treatment (Fig. 2*B*). Despite this growth advantage in vitro, however, the mutant strain was comparable with WT *Mtb* with respect to killing THP-1 macrophage cells (Fig. S1).

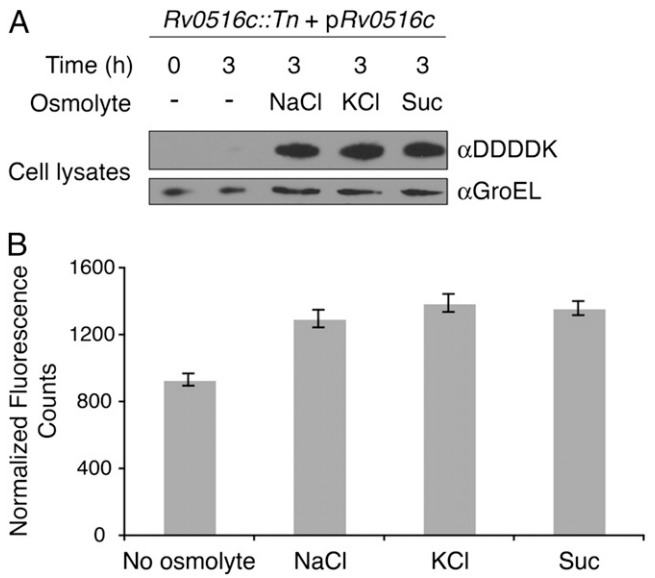

Fig. 1. *Rv0516c* is induced by osmotic stress. (*A*) Western blot analysis of Rv0516c expression in *Mtb* after treatment with 140 mM sodium chloride (NaCl), 140 mM potassium chloride (KCl), 280 mM sucrose (Suc), or no osmolyte for 3 h. GroEL, an intracellular molecular chaperone, was detected as a loading control. (*B*) Mean fluorescence intensity of *Mtb* expressing GFP under the control of the *Rv0516c* promoter after treatment with 140 mM NaCl, 140 mM KCl, 280 mM Suc, or no osmolyte for 2 d. These data represent the mean ± SD of three independent cultures. $P < 0.02$ for all conditions relative to control (i.e., no osmolyte).

***Rv0516c* Disruption Increases Resistance to Several PG Biosynthesis Inhibitors and Also Decreases PG Thickness.** The enhanced resistance of the *Rv0516c* mutant to osmotic stress suggested that *Rv0516c* might affect cell wall integrity. Accordingly, we evaluated the sensitivity of the mutant strain to various forms of cell wall stress. We determined the minimal inhibitory concentrations (MICs) of isoniazid (an inhibitor of fatty and mycolic acid biosynthesis) (43), SDS, and the PG biosynthesis inhibitors D-cycloserine and vancomycin (Fig. 2*D*). Vancomycin was the only compound that exhibited a different MIC for the mutant strain; the MIC was fourfold higher for *Rv0516c::Tn* than WT or complemented *Mtb*. Strikingly, the cfus produced by *Rv0516c::Tn* after incubation with 1.5 μg/mL vancomycin exceeded the cfus of the WT strain by approximately three orders of magnitude, whereas complementation conferred WT cfu levels (Fig. 2*E*). In contrast, D-cycloserine, which blocks PG biosynthesis by inhibiting D-/L-alanine racemase as well as D-alanine:D-alanine ligase (44), was equally effective at suppressing growth of the WT and mutant strains (Fig. 2*D*). These data suggest that *Rv0516c* may regulate a late stage of PG assembly that is inhibited by vancomycin. To further explore this hypothesis, we tested two β-lactam antibiotics, penicillin and ampicillin, that block the formation of peptide cross-links in PG. We observed a two- and threefold increase in the MICs of penicillin and ampicillin, respectively, for *Rv0516c::Tn* relative to WT *Mtb* in the presence of 5 μg/mL clavulanic acid, a β-lactamase inhibitor (Table S1) (45). Taken together, these data suggest that *Rv0516c* may modulate PG cross-linking or alternatively, increase *Mtb* susceptibility to these antibiotics by enhancing drug access to the cell wall.

The link between *Rv0516c* and PG biosynthesis suggested by our MIC data led us to consider a role for the gene in modulating PG structure. Using transmission EM (TEM), we measured the PG thickness of WT, *Rv0516c::Tn*, and complemented cells. The average PG thickness of the mutant strain was ~25% less than the average PG thickness of the WT strain, a phenotype partially reversed by complementation (Fig. 2 *F* and *G*). Notably, our measurements for PG thickness of WT *Mtb* are comparable with previously reported values (46).

Rv0516c Suppresses the Transcriptional Response to Osmotic Stress by Regulating SigF. To determine how Rv0516c might influence *Mtb* physiology and cell wall architecture in response to osmotic stress, we searched for sequence-based functional clues. Bioinformatics provided the first indication that Rv0516c might operate in a transcriptional capacity, because it shares significant homology with SpoIIAA, an anti-anti–σ-factor from *B. subtilis* (Fig. 3*A*) (47). Encouragingly, Rv0516c was previously shown to interact with the *Mtb* alternative σ-factor SigF in a yeast two-hybrid assay (48), and SigF has been implicated in regulating cell

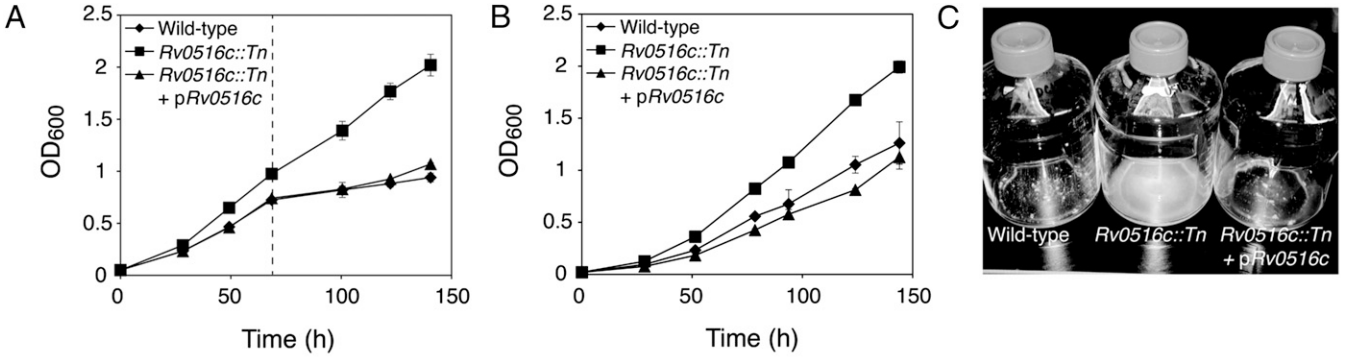

D

MIC[a]	Wild-type	*Rv0516c::Tn*	*Rv0516c::Tn* + p*Rv0516c*
Isoniazid (μg/mL)	0.0313	0.0313	0.016
SDS (%, v/v)	0.01	0.01	0.01
D-Cycloserine (μg/mL)	3.9	3.9	3.9
Vancomycin (μg/mL)	0.78	3.13	0.78

[a]Minimal inhibitory concentration. MIC values represent the lowest concentration of drug that visibly inhibited growth of the indicated strain after 1 or 2 weeks. These values were consistent among 3 biological replicates.

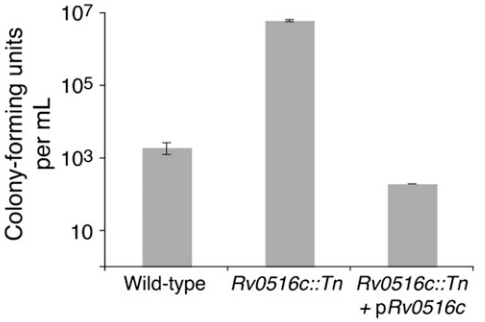

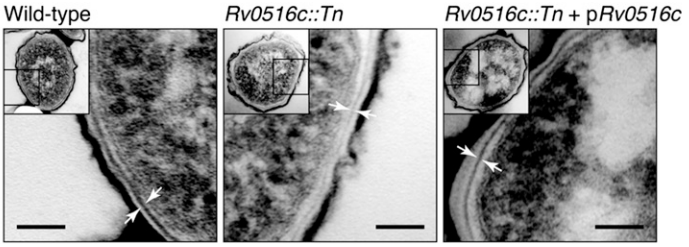

G

Strain	PG Thickness (nm)[a]
Wild-type	4.6 ± 0.8
Rv0516c::Tn	3.5 ± 0.7
Rv0516c::Tn + p*Rv0516c*	4.1 ± 0.6

[a]Average PG thickness was calculated via blind analysis of PG measurements taken from 20-21 cells of each strain. $P < 0.00002$ for wild-type and *Rv0516c::Tn*; $P < 0.005$ for *Rv0516c::Tn* and *Rv0516c::Tn* + p*Rv0516c*; $P < 0.02$ for wild-type and *Rv0516c::Tn* + p*Rv0516c*.

Fig. 2. *Rv0516c* disruption enhances resistance to osmotic stress and the PG biosynthesis inhibitor vancomycin and decreases PG thickness. In vitro growth kinetics of WT (◆), *Rv0516c::Tn* (■), and complemented *Mtb* (▲) strains (*A*) before and after treatment with 0.5 M NaCl (denoted by the dotted line) and (*B*) in the absence of NaCl treatment. These data represent the mean ± SD of three independent cultures. (*C*) WT, *Rv0516c::Tn*, and complemented *Mtb* strains grown to early stationary phase in Middlebrook 7H9 medium and treated with 0.5 M NaCl for 3 d. (*D*) MICs of various cell wall-perturbing agents calculated from three biological replicates. (*E*) Cfus of WT, *Rv0516c::Tn*, and complemented *Mtb* strains treated with 1.5 μg/mL vancomycin for 4 d. These results represent the mean ± SD of two biological replicates. (*F*) Representative TEM images of WT, *Rv0516c::Tn*, and complemented cells. The PG layer of the cell wall is denoted by two white arrows. *Insets* show the region of the cell that has been magnified. (Scale bars: 50 nm.) (*G*) Average PG thickness of WT, *Rv0516c::Tn*, and complemented strains determined by TEM. These data represent the mean ± SD calculated from the blind analysis of 20–21 cells per strain.

wall composition and morphology (49, 50). Indeed, *Rv0516c* itself is transcriptionally regulated by SigF (49), and RT-PCR analysis has previously shown that *Rv0516c* transcript levels increase after NaCl treatment (51), which is consistent with our microarray data. Moreover, the promoter region of *Rv0516c*, which is sufficient to induce GFP expression in response to osmotic stress (Fig. 1*B*), contains elements of the SigF recognition motif (49). Therefore, we postulated that osmotic stress activates SigF-mediated transcription, which is, in turn, regulated by Rv0516c expression.

We compared the transcriptional profiles of *Rv0516c::Tn* and WT *Mtb* after NaCl treatment (Table 1 and Datasets S1–S3) and discovered that many genes were more up- or down-regulated by osmotic stress in the mutant strain (Datasets S4 and S5) (National Center for Biotechnology Information/Gene Expression Omnibus accession no. GSE50160). Notably, transcription of the *arg* and *Rv3616c-Rv3614c* operons, which comprise some of the most highly induced genes from the WT strain, increased approximately two- to fourfold in *Rv0516c::Tn* (Fig. 3*B*). These findings suggest that *Rv0516c* disruption enhances the transcriptional response of *Mtb* to osmotic stress. Thus, despite the predicted structural homology of Rv0516c to SpoIIAA, the transcriptional profile of *Rv0516c::Tn* is more consistent with the transcriptional profile of a σ-factor antagonist mutant. As well, we identified several SigF-regulated genes (49, 50, 52) that were more highly induced in the *Rv0516c* mutant (Table 2). These data also support a role for Rv0516c in inhibiting SigF activity. Given the significant influence of Rv0516c on the transcriptional and physiological responses of *Mtb* to osmotic stress, we have renamed this protein osmosensory protein A (OprA).

Phosphorylation of OprA by PknD Is Required for *oprA* Induction in Response to Osmotic Stress. We next sought to identify the mechanism by which OprA expression responds to changes in extracellular osmolarity. Because phosphorylation of anti- and anti-anti–σ-factors is a well-established mechanism of alternative σ-factor regulation (10, 11, 24), we hypothesized that phosphorylation of OprA might affect its expression. Interestingly, transcription of *oprA* and other SigF-regulated genes is altered by overexpression of the membrane-associated STPK PknD (34). Furthermore, PknD has been shown to directly phosphorylate OprA at Thr2 in

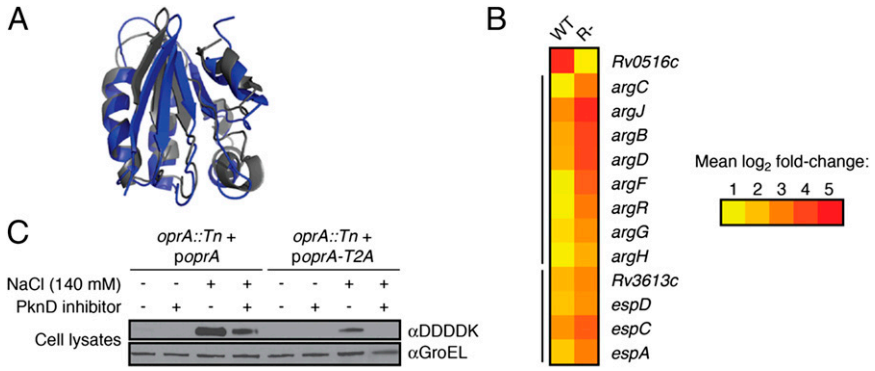

Fig. 3. Rv0516c regulates transcription of osmotically activated genes and is regulated by PknD under osmotic stress. (*A*) The predicted protein fold of Rv0516c (gray) determined by the modeling program Phyre (47) using the crystal structure of the anti-anti–σ-factor SpoIIAA from *B. subtilis* (blue) as a template. (*B*) Heat map depicting the relative transcription of *arg* and *Rv3616c-Rv3613c* genes in WT and *Rv0516c::Tn* (R-) *Mtb* after treatment with 140 mM NaCl for 1 h. Changes in gene expression are relative to untreated WT or R- cells, respectively, and represent the average of four biological replicates (details in *Materials and Methods*). The mean fold change in expression of each gene ($\log_2$ scale) is indicated by the corresponding color. Yellow represents a twofold increase in expression. Red represents a 32-fold increase in expression. All changes in expression are statistically significant. Black bars to the left of the map denote probable operons. (*C*) Western blot analysis of OprA (Rv0516c) and a phosphorylation-deficient OprA mutant (*oprA::Tn* + p*oprA-T2A*) after exposure to 140 mM NaCl and/or 60 μM PknD inhibitor (SP600125). GroEL was detected as a loading control.

Mtb (34). We considered the possibility that transcription of *oprA* is modulated by phosphorylation of the corresponding protein. If so, phosphorylation of OprA may be required for its transcriptional activation by osmotic stress.

To explore this possibility, we expressed a phosphorylation-deficient (T2A) variant of OprA under the control of the native promoter in the mutant strain (*oprA::Tn* + p*oprA-T2A*). Compared with expression of the WT protein, expression of the T2A OprA mutant reduced *oprA* induction in response to osmotic stress (Fig. 3*C*, compare lanes 3 and 7). In a complementary experiment, we observed that treatment of cells with a PknD-selective small-molecule inhibitor (34) blunted expression of OprA under osmotic stress (Fig. 3*C*, compare lanes 3 and 4). These data suggest that PknD phosphorylation on Thr2 inactivates OprA and stimulates SigF-dependent expression of *oprA* in response to increasing osmolarity.

We also considered whether phosphorylation, in addition to activating OprA expression, might mediate a direct interaction between OprA and SigF. Indeed, other alternative σ-factor binding proteins have been shown to interact with their targets in a phosphorylation-dependent manner (10, 53). Using affinity chromatography and SDS/PAGE analysis, we sought to determine whether OprA, in either a phosphorylated or unphosphorylated state, binds to SigF in vitro (*SI Materials and Methods*). However, we were unable to detect robust complex formation, suggesting that these proteins interact transiently or that their connection is indirect and involves additional proteins. Alternatively, OprA could be an upstream regulator of SigF activity.

Table 2. SigF-regulated genes more highly induced by 140 mM NaCl in *Rv0516c::Tn*

Gene number	Annotation*	Description*	Fold change†	Ref.
Rv0035	*fadD34*	Probable fatty acid-CoA ligase	3.2	49
Rv1172c	*PE12*	PE family protein	2.5	50
Rv1252c	*lprE*	Probable lipoprotein	2.1	50
Rv1284	*canA*	β-Carbonic anhydrase	2	50
Rv1379	*pyrR*	Probable pyrimidine operon regulatory protein	2.5	49
Rv1380	*pyrB*	Probable aspartate carbamoyltransferase	2.1	49
Rv1441c	*PE_PGRS26*	PE-PGRS family protein	2.2	50
Rv1652‡	*argC*	Probable *N*-acetyl-γ-glutamyl-phosphate reductase	3.5	50
Rv2140c	*TB18.6*	Conserved hypothetical protein	2.1	52
Rv2400c	*subI*	Probable sulfate binding lipoprotein	2.7	50
Rv2428	*ahpC*	Alkyl hydroperoxide reductase C	3.3	49
Rv3136	*PPE51*	PPE family protein	2.2	50
Rv3559c		Probable oxidoreductase	2.5	49
Rv3615c‡	*espC*	ESX-1 secretion-associated protein	1.8	49
Rv3914	*trxC*	Thioredoxin	2.1	49

DNA microarray analysis was used to identify *Mtb* genes that were significantly induced or repressed in WT *Mtb* strain CDC1551 and *Rv0516c::Tn* after a 1-h exposure to 140 mM NaCl. Arrays from four biological replicates were analyzed using SAM (36). Genes having a mean $\log_2$ fold change of one or greater with an SAM-assigned q value of <0.06% were deemed significant. Genes that were more highly induced in *Rv0516c::Tn* than WT *Mtb* (fold change ≥ 2) and have previously been shown to be regulated by SigF are summarized here.

*Gene annotations and descriptions were obtained from TubercuList (http://tuberculist.epfl.ch/) and the J. Craig Venter Institute Comprehensive Microbial Resource (http://cmr.jcvi.org/cgi-bin/CMR/CmrHomePage.cgi).

†Fold change increase in gene expression in *Rv0516c::Tn* relative to WT.

‡Up-regulated in both WT and *Rv0516c::Tn*.

OprA and PknD Selectively Regulate Expression and Secretion of the Type VII ESX-1 Effector Protein EspA. *Rv3616c*, another gene induced by osmotic stress, encodes a virulence-associated substrate of the type VII ESX-1 secretion system, EspA (40, 54). EspA has been proposed to enhance cell wall integrity (54) and may be protective against conditions of osmotic stress. As well, *espA* resides in the same operon as the SigF-regulated gene *Rv3615c* (49, 55), which itself is induced by osmotic stress (Table 1). Therefore, we explored the relationship between EspA and increasing osmolarity in more detail. We evaluated EspA levels in WT *Mtb* cell lysates and observed a marked increase in EspA abundance after NaCl treatment (Fig. 4*A*). Interestingly, expression of ESAT-6, another substrate of the ESX-1 secretion system, was unaffected by osmotic stress. An increase in EspA but not ESAT-6 levels was also observed on exposure of *Mtb* to other osmolytes (Fig. S2), suggesting that osmotic stress has a differential effect on the abundance of ESX-1 substrates.

Because *espA* was induced more by osmotic stress in the *oprA* mutant, we hypothesized that OprA might influence EspA expression. To investigate this possibility, we compared EspA expression and secretion in *oprA::Tn* vs. WT *Mtb* in the presence or absence of osmotic stress. Although *espA* was still induced by NaCl treatment in *oprA::Tn*, EspA secretion was substantially diminished (Fig. 4*A*). Remarkably, this phenotype was independent of culture osmolarity and specific to EspA, because no change in ESAT-6 secretion was observed in the mutant strain, despite the codependent secretion of these proteins (40, 54, 56).

Furthermore, we observed a sharp decrease in EspA expression in the absence of OprA phosphorylation at Thr2 (Fig. 4*B*), whereas ESAT-6 levels remained unchanged. The apparent link between OprA phosphorylation and EspA expression prompted us to evaluate whether inhibition of PknD activity might also correlate with reduced EspA levels. As anticipated, treatment with the selective PknD inhibitor (34) diminished EspA expression in both the presence and absence of osmotic stress (Fig. 4*C*). Moreover, PknD inhibition seemed to reduce EspA secretion, particularly in response to NaCl treatment. Again, the expression and secretion of ESAT-6 were unaffected by exposure to osmotic stress or treatment with the PknD inhibitor. In sum, these findings suggest that OprA and PknD selectively regulate EspA expression and secretion.

Discussion

In light of these data, we propose a model for an osmosensory pathway that regulates *Mtb* adaptation to osmotic stress (Fig. 5). The pathway commences with PknD, which is activated by an increase in extracellular osmolarity and subsequently, phosphorylates OprA on Thr2. OprA phosphorylation enables SigF binding to RNA polymerase, which promotes transcription of *oprA*, *espA*, and other genes associated with changes in *Mtb* cell wall structure and metabolism. SigF activation could occur indirectly by regulation of an environmental phosphatase that controls alternative σ-factors (34) or directly by release from a noncanonical OprA complex (Fig. 5) (48). Although induction of *oprA* by osmotic stress seems contrary to the encoded protein's inhibition of SigF activity, such negative feedback is likely required to prevent prolonged induction of energetically taxing metabolic pathways (e.g., protein biosynthesis) and immunogenic virulence factors (e.g., EspA) (54) that may compromise bacterial survival in the host.

The OprA osmosensory pathway, with its dependence on both an STPK family member and an alternative σ-factor, stands apart from previously characterized bacterial responses to environmental stress. TCSs, the primary agents of stress-induced signal transduction in bacteria, typically comprise a single membrane-associated histidine kinase and cytosolic response regulator (3). Some TCSs have been shown to respond to osmotic stress (29–31, 57, 58), and a few of these systems are thought to have counterparts in *Mtb* (59, 60). Alternative σ-factors have also been shown to modulate bacterial transcription in response to diverse environmental cues and are often regulated by anti–σ-factors with kinase activity (7, 61). By contrast, the OprA osmosensory pathway represents a fundamentally unique transcriptional circuit, in which a eukaryotic-like STPK stimulates gene expression by regulating alternative σ-factor activity in response to osmotic stress. As a result, this pathway merges eukaryotic and prokaryotic mechanisms of signal transduction, establishing a unique paradigm for bacterial detection of environmental stress.

Although these studies suggest that osmotic stress activates PknD, the biochemical basis of this response remains unknown. Osmolytes may induce a change in the extracellular domain of PknD (62, 63) that stimulates the intracellular kinase domain. Alternatively, PknD may be particularly sensitive to the membrane destabilizing effects of osmotic stress, which could trigger kinase activation. A third possibility is that increasing osmolarity promotes the release of PG fragments that may bind to and activate PknB, which has been shown to phosphorylate the kinase domain of PknD (64).

Despite the predicted structural homology between OprA and the anti-anti–σ-factor SpoIIAA, our data are more consistent with classification of OprA as an SigF antagonist. First, OprA seems to repress several genes regulated by osmotic stress and/or SigF (Fig. 3*B* and Table 2) that may be protective against increasing osmolarity and inhibitors of PG biosynthesis. For example, osmotically activated genes that facilitate protein translation or folding or mitigate oxidative stress are more highly induced on *oprA* disruption (Table 2 and Dataset S4). Furthermore, *pbpB* (*Rv2163c*), a putative transpeptidase involved in PG biosynthesis, and *amiC* (*Rv2888c*), a putative PG hydrolase involved in septal cleavage, are only up-regulated by osmotic stress in the *oprA*

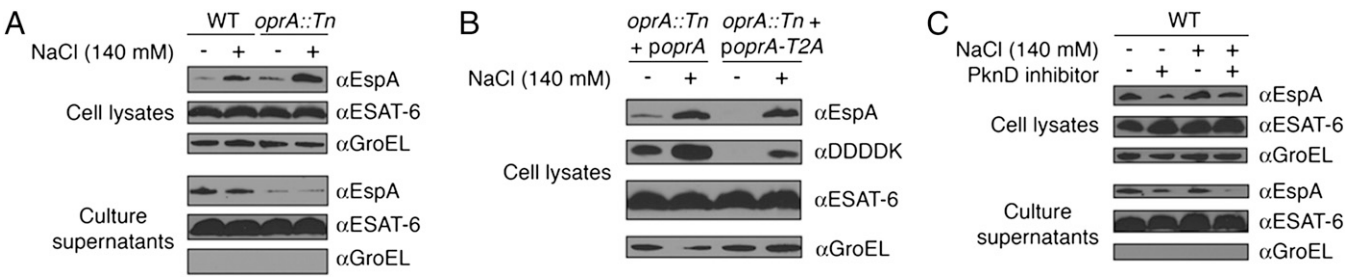

Fig. 4. Osmotic stress, OprA, and PknD regulate expression and secretion of the ESX-1–associated virulence factor EspA. (*A*) Western blot analysis of EspA abundance in cell lysates and culture supernatants of WT and *oprA::Tn Mtb* after exposure to 140 mM NaCl. Protein levels of ESAT-6, another substrate of the ESX-1 secretion system, and GroEL are also shown. (*B*) Western blot analysis of EspA and OprA (anti-DDDDK) abundance in cells expressing WT (*oprA::Tn* + p*oprA*) and phosphorylation-deficient OprA (*oprA::Tn* + p*oprA-T2A*) after exposure to 140 mM NaCl. (*C*) Western blot analysis of EspA abundance in WT *Mtb* after exposure to 140 mM NaCl and/or 60 μM PknD inhibitor (SP600125).

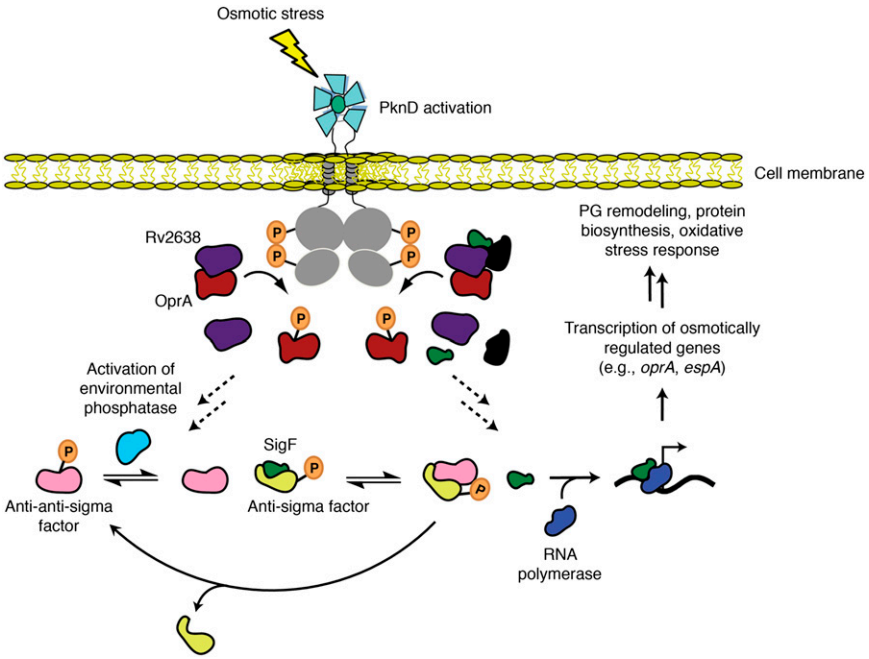

Fig. 5. Model of the OprA osmosensory pathway. Osmotic stress activates PknD phosphorylation of OprA, which stimulates the release of SigF from an inhibitory complex and enables the transcription of osmotically regulated genes, such as *oprA* and *espA*. This transcriptional response pathway mediates changes in *Mtb* metabolism and cell wall structure. The mechanism of SigF activation remains unknown. Unphosphorylated OprA forms a complex with the anti-anti–σ-factor paralog Rv2638 that dissociates on OprA phosphorylation (34). Dissociation of this complex may stimulate an environmental phosphatase that dephosphorylates an anti-anti–σ-factor, facilitating the release of SigF from a cognate anti–σ-factor. SigF subsequently binds RNA polymerase, enabling transcription of genes required for the osmotic stress response. The anti–σ-factor can, in turn, phosphorylate the anti-anti–σ-factor to reinitiate the cycle of SigF inhibition. Alternatively, Rv2638 and OprA may form a noncanonical complex with SigF and other SigF-associated regulators that dissociates on OprA phosphorylation, allowing SigF to bind RNA polymerase.

mutant (Dataset S4). These genes may contribute to the improved antibiotic resistance and markedly reduced PG thickness of the mutant strain (Fig. 2 *E* and *G*). Second, PknD overexpression stimulates OprA phosphorylation and SigF-dependent transcription (34). Our proposed model is consistent with the regulatory framework in which OprA antagonizes SigF, because phosphorylation of OprA relieves inhibition of SigF activity. Third, unlike the SpoIIAA phosphorylation site, which is at the base of an α-helix in a highly structured region of the protein (65), the OprA phosphorylation site occurs in a presumably unstructured N-terminal region that is excluded from the SpoIIAA-derived homology model (Fig. 3*A*). Our results reveal that this phosphorylation functionally inhibits OprA.

The biochemical effect of OprA phosphorylation remains an open question. Phosphorylation may directly modulate the binding of OprA to other proteins or stabilize the unstructured N-terminal region of OprA, thereby preventing premature proteolytic degradation. PknB-dependent phosphorylation of RseA, the anti–σ-factor of SigE, has been shown to stimulate RseA proteolysis by ClpC in *M. smegmatis* (66). In *Mtb*, the transcriptional regulator ClgR (Rv2745c) induces transcription of the *clpC* operon (67, 68). Interestingly, ClgR is up-regulated by osmotic stress (Table 1), suggesting that a similar proteolytic mechanism may control OprA activity.

OprA may interact with a complex network of proteins to integrate the bacterial response to osmotic stress. For example, OprA has been shown to bind another anti-anti–σ-factor homolog, Rv2638 (34, 48). This interaction is blocked in vitro by OprA phosphorylation (34). Typically, members of this protein family either directly regulate anti–σ-factors (9) or the environmental phosphatase that antagonizes anti–σ-factor activity (11). However, only those homologs that regulate the environmental phosphatase have been shown to interact with each other (69). In *B. subtilis*, these regulators form a multiprotein complex called the stressosome (70). OprA and Rv2638 may be part of a similar complex in *Mtb* that indirectly stimulates SigF activity through regulation of an environmental phosphatase. Alternatively, Rv2638 could serve as an intermediary between different SigF-associated regulators. A previously characterized anti-anti–σ-factor of SigF, RsfA (71), and the cognate anti–σ-factor, UsfX (72), seem to interact with Rv2638 but not OprA in a yeast two-hybrid assay (48). These proteins may form a noncanonical complex with OprA that controls SigF activity. Other osmotically induced transcription factors (e.g., WhiB1 and ClgR) (Table 1) may also play a role in regulating bacterial osmoadaptation independent of OprA.

In sum, our data implicate OprA as the nexus of an *Mtb* osmosensory pathway. As well, we discovered a role for PknD in adaptation to osmotic stress, linking this STPK family member to specific transcriptional and physiological responses. Finally, we have shown the selective environmental regulation of a type VII ESX-1 substrate. The complex network of proteins comprising the OprA pathway may represent opportunities for modulating the cell wall structure and antibiotic susceptibility of this global human pathogen. Notably, growth of *Streptococcus pyogenes* in high salt concentrations is STPK-dependent, suggesting an osmosensory role for another bacterial receptor kinase (73). Given the widespread occurrence of eukaryotic-like STPKs in prokaryotes, these receptors may also contribute to osmosensing in other organisms.

Materials and Methods

Bacterial Strains and Plasmids. Tables S2–S4 contain complete lists of the strains, plasmids, and primers, respectively, used in this study. Details of plasmid construction can be found in *SI Materials and Methods*. *Mtb* strains CDC1551 and *Rv0516c::Tn*, a CDC1551 mutant with a *Himar1* transposon insertion after the first 101 bp of the *Rv0516c* gene (74), were obtained from the Tuberculosis Animal Research and Gene Evaluation Taskforce (National

Institutes of Health/National Institute of Allergy and Infectious Diseases contract no. N01 AI-30036).

Growth Conditions and Media. *Mtb* strain CDC1551 and its derivatives were grown in Middlebrook 7H9 or Sauton's medium or on Middlebrook 7H11 solid agar with the appropriate antibiotics. Detailed media formulations can be found in *SI Materials and Methods*. Unless otherwise indicated, cultures were grown in roller bottles or aerated shaker flasks at 37 °C.

Sample Preparation for Microarray and Western Blot Analysis. *Mtb* cultures prepared from frozen glycerol stocks were grown to midlog phase in 7H9 medium, washed, passaged one time in Sauton's medium, and then grown for 2 d to early log phase. For microarray analysis, a single culture was split into two equal parts: one part was immediately harvested and frozen on dry ice, and the second part was treated with a small volume of concentrated NaCl in Sauton's medium (140 mM final concentration for an increase in osmolarity of ∼280 mOsm/L). This culture was incubated for 1 h at 37 °C before harvesting and freezing the cells exactly as previously described. For Western blot analysis, cultures were treated with osmolyte (140 mM NaCl, 140 mM KCl, or 280 mM sucrose for an increase in osmolarity of ∼280 mOsm/L) for 3 h, harvested by centrifugation, and lysed as previously described (40). Culture supernatants were sterilized two times by filtration, concentrated, and stored at −20 °C. Total protein concentrations were determined by Bradford assay (Bio-Rad) and normalized before SDS/PAGE.

RNA Extraction and Microarray Analysis. RNA extraction and microarray analysis were performed as previously described (75). Whole-genome *Mtb* arrays were provided by the Pathogen Functional Genomics Resource Center (National Institute of Allergy and Infectious Diseases contract no. N01 AI-15447). Arrays were scanned with a GenePix 4000B scanner and analyzed using GenePix 6.0 and Acuity 4.1 software. Lowess-normalized data from four biological replicates were analyzed using the Significance Analysis of Microarrays (SAM) program (36). Genes with a mean $\log_2$ fold change of at least one with a false discovery rate value (i.e., q value) of <0.06% were deemed significant.

Antibodies. Primary antibodies against ESAT-6, GroEL, and the DDDDK tag were from Abcam. The EspA antibody (rabbit polyclonal serum) was a gift from S. Fortune at Harvard University, Cambridge, MA. HRP-conjugated secondary antibodies were detected using chemiluminescent reagents (Pierce). Antibody details are provided in *SI Materials and Methods*.

GFP Reporter Assays. *Mtb* strain CDC1551 transformed with p*Rv0516c-gfp* was grown to midlog phase in 7H9 medium, washed, passaged one time in Sauton's medium, and then grown for 2 d to early log phase. Aliquots of this culture (10 mL each) were then transferred to 50-mL conical tubes and treated with a small volume of concentrated NaCl, KCl, or sucrose in Sauton's medium to a final concentration of 140 mM (NaCl or KCl) or 280 mM (sucrose) for an increase in osmolarity of ∼280 mOsm/L. After 2 d at 37 °C with shaking, the total fluorescence of fixed cells from triplicate cultures was measured and normalized by cell density.

In Vitro Growth Studies. Bacteria were inoculated in 7H9 medium (OD_{600} of 0.05) in aerated shaker flasks. At midlog phase, cultures were treated with a small volume of concentrated NaCl in 7H9 medium (0.5 M final concentration for an increase in osmolarity of ∼1 Osm/L) for 3 d. A second set of cultures was similarly prepared but grown in the absence of NaCl.

Cell Wall Stress Resistance Assays. MICs were determined using the broth microdilution method essentially as previously described (76). To evaluate vancomycin resistance, bacteria were grown for 3 d in 7H9 medium with 1.5 μg/mL vancomycin and plated on 7H11 agar plates for the enumeration of cfus.

TEM Analysis. *Mtb* cells were prepared by formaldehyde fixation (77) and analyzed by TEM as previously described (78, 79). Measurements were taken with Maxim DL software.

Structural Modeling. The protein structure of Rv0516c was modeled using the freely available PHYRE Protein Fold Recognition server (www.sbg.bio.ic.ac.uk/∼phyre/) (47). The estimated precision value of the SpoIIAA protein from *B. subtilis* (Protein Data Bank ID code 1AUZ) was 100%. MacPyMOL was used to align the Rv0516c model with the structure of SpoIIAA.

PknD Inhibition Assays. Bacteria grown in Sauton's medium were treated with 60 μM SP600125 (InSolution JNK Inhibitor II; EMD Chemicals), a JNK inhibitor that has been previously shown to specifically inhibit phosphorylation by the STPK PknD for at least 8 h at this concentration (34). After 2 h at 37 °C, cells were treated with a small volume of concentrated NaCl in Sauton's medium (140 mM final concentration for an increase in osmolarity of ∼280 mOsm/L) for an additional 3 h. Cell lysates and culture supernatants were prepared as previously described.

Detailed protein preparation, assay, and TEM procedures are described in *SI Materials and Methods*.

ACKNOWLEDGMENTS. We thank K. Sogi and L. Prach for technical contributions, D. Portnoy and J. Doudna for equipment, and J. Seeliger, S. Gilmore, S. Fortune, A. Mandlik, A. Greenstein, M. Boyce, and members of the C.R.B. laboratory for helpful discussions. M.S.S. was supported by American Cancer Society Postdoctoral Fellowship 119087-PF-10-258-01-MPC. C.O. is a recipient of the American Society of Microbiology Robert D. Watkins Graduate Research Fellowship and the Bank of America Endowed Minority Fellowship. C.G. was supported by Paul G. Allen Family Foundation Grant 8999, the American Lung Association, and University of Washington Center for AIDS Research New Investigator Award P30AI027757, which was through a National Institutes of Health-funded program. We received funding from National Institutes of Health Grants R01GM70962 (to T.A.), P01AI095208 (to T.A.), and AI51622 (to C.R.B.).

1. Poole K (2012) Bacterial stress responses as determinants of antimicrobial resistance. *J Antimicrob Chemother* 67(9):2069–2089.
2. Nathan C (2012) Fresh approaches to anti-infective therapies. *Sci Transl Med* 4(140): 140sr2.
3. Jung K, Fried L, Behr S, Heermann R (2012) Histidine kinases and response regulators in networks. *Curr Opin Microbiol* 15(2):118–124.
4. Hoch JA (2000) Two-component and phosphorelay signal transduction. *Curr Opin Microbiol* 3(2):165–170.
5. Staroń A, et al. (2009) The third pillar of bacterial signal transduction: Classification of the extracytoplasmic function (ECF) sigma factor protein family. *Mol Microbiol* 74(3): 557–581.
6. Bashyam MD, Hasnain SE (2004) The extracytoplasmic function sigma factors: Role in bacterial pathogenesis. *Infect Genet Evol* 4(4):301–308.
7. Hughes KT, Mathee K (1998) The anti-sigma factors. *Annu Rev Microbiol* 52:231–286.
8. Helmann JD (1999) Anti-sigma factors. *Curr Opin Microbiol* 2(2):135–141.
9. Campbell EA, Westblade LF, Darst SA (2008) Regulation of bacterial RNA polymerase sigma factor activity: A structural perspective. *Curr Opin Microbiol* 11(2):121–127.
10. Igoshin OA, Price CW, Savageau MA (2006) Signalling network with a bistable hysteretic switch controls developmental activation of the sigma transcription factor in *Bacillus subtilis*. *Mol Microbiol* 61(1):165–184.
11. Kim TJ, Gaidenko TA, Price CW (2004) In vivo phosphorylation of partner switching regulators correlates with stress transmission in the environmental signaling pathway of *Bacillus subtilis*. *J Bacteriol* 186(18):6124–6132.
12. Raven JF, Koromilas AE (2008) PERK and PKR: Old kinases learn new tricks. *Cell Cycle* 7(9):1146–1150.
13. Seta KA, Spicer Z, Yuan Y, Lu G, Millhorn DE (2002) Responding to hypoxia: Lessons from a model cell line. *Sci STKE* 2002(146):re11.
14. Ferretti AC, Larocca MC, Favre C (2012) Nutritional stress in eukaryotic cells: Oxidative species and regulation of survival in time of scarceness. *Mol Genet Metab* 105(2): 186–192.
15. Pereira SF, Goss L, Dworkin J (2011) Eukaryote-like serine/threonine kinases and phosphatases in bacteria. *Microbiol Mol Biol Rev* 75(1):192–212.
16. Av-Gay Y, Everett M (2000) The eukaryotic-like Ser/Thr protein kinases of *Mycobacterium tuberculosis*. *Trends Microbiol* 8(5):238–244.
17. Greenstein AE, et al. (2005) Structure/function studies of Ser/Thr and Tyr protein phosphorylation in *Mycobacterium tuberculosis*. *J Mol Microbiol Biotechnol* 9(3–4): 167–181.
18. Molle V, Kremer L (2010) Division and cell envelope regulation by Ser/Thr phosphorylation: Mycobacterium shows the way. *Mol Microbiol* 75(5):1064–1077.
19. Kang CM, et al. (2005) The *Mycobacterium tuberculosis* serine/threonine kinases PknA and PknB: Substrate identification and regulation of cell shape. *Genes Dev* 19(14): 1692–1704.
20. Gee CL, et al. (2012) A phosphorylated pseudokinase complex controls cell wall synthesis in mycobacteria. *Sci Signal* 5(208):ra7.
21. Kang CM, Nyayapathy S, Lee JY, Suh JW, Husson RN (2008) Wag31, a homologue of the cell division protein DivIVA, regulates growth, morphology and polar cell wall synthesis in mycobacteria. *Microbiology* 154(Pt 3):725–735.
22. Mir M, et al. (2011) The extracytoplasmic domain of the *Mycobacterium tuberculosis* Ser/Thr kinase PknB binds specific muropeptides and is required for PknB localization. *PLoS Pathog* 7(7):e1002182.
23. Sajid A, et al. (2011) Interaction of *Mycobacterium tuberculosis* elongation factor Tu with GTP is regulated by phosphorylation. *J Bacteriol* 193(19):5347–5358.
24. Park ST, Kang CM, Husson RN (2008) Regulation of the SigH stress response regulon by an essential protein kinase in *Mycobacterium tuberculosis*. *Proc Natl Acad Sci USA* 105(35):13105–13110.

25. Shah IM, Laaberki MH, Popham DL, Dworkin J (2008) A eukaryotic-like Ser/Thr kinase signals bacteria to exit dormancy in response to peptidoglycan fragments. *Cell* 135(3): 486–496.
26. Squeglia F, et al. (2011) Chemical basis of peptidoglycan discrimination by PrkC, a key kinase involved in bacterial resuscitation from dormancy. *J Am Chem Soc* 133(51): 20676–20679.
27. Pompeo F, et al. (2012) Phosphorylation of CpgA protein enhances both its GTPase activity and its affinity for ribosome and is crucial for *Bacillus subtilis* growth and morphology. *J Biol Chem* 287(25):20830–20838.
28. Price CT, Bukka A, Cynamon M, Graham JE (2008) Glycine betaine uptake by the ProXVWZ ABC transporter contributes to the ability of *Mycobacterium tuberculosis* to initiate growth in human macrophages. *J Bacteriol* 190(11):3955–3961.
29. Sleator RD, Hill C (2002) Bacterial osmoadaptation: The role of osmolytes in bacterial stress and virulence. *FEMS Microbiol Rev* 26(1):49–71.
30. Csonka LN (1989) Physiological and genetic responses of bacteria to osmotic stress. *Microbiol Rev* 53(1):121–147.
31. Sleator RD, Hill C (2005) A novel role for the LisRK two-component regulatory system in listerial osmotolerance. *Clin Microbiol Infect* 11(8):599–601.
32. Porter ME, Dorman CJ (1994) A role for H-NS in the thermo-osmotic regulation of virulence gene expression in *Shigella flexneri*. *J Bacteriol* 176(13):4187–4191.
33. Gao H, et al. (2011) Phenotypic and transcriptional analysis of the osmotic regulator OmpR in *Yersinia pestis*. *BMC Microbiol* 11:39.
34. Greenstein AE, et al. (2007) *M. tuberculosis* Ser/Thr protein kinase D phosphorylates an anti-anti-sigma factor homolog. *PLoS Pathog* 3(4):e49.
35. Bourque CW (2008) Central mechanisms of osmosensation and systemic osmoregulation. *Nat Rev Neurosci* 9(7):519–531.
36. Tusher VG, Tibshirani R, Chu G (2001) Significance analysis of microarrays applied to the ionizing radiation response. *Proc Natl Acad Sci USA* 98(9):5116–5121.
37. Xu Y, Labedan B, Glansdorff N (2007) Surprising arginine biosynthesis: A reappraisal of the enzymology and evolution of the pathway in microorganisms. *Microbiol Mol Biol Rev* 71(1):36–47.
38. Xu S, Zhou J, Liu L, Chen J (2011) Arginine: A novel compatible solute to protect *Candida glabrata* against hyperosmotic stress. *Process Biochem* 46(6):1230–1235.
39. MacGurn JA, Raghavan S, Stanley SA, Cox JS (2005) A non-RD1 gene cluster is required for Snm secretion in *Mycobacterium tuberculosis*. *Mol Microbiol* 57(6):1653–1663.
40. Fortune SM, et al. (2005) Mutually dependent secretion of proteins required for mycobacterial virulence. *Proc Natl Acad Sci USA* 102(30):10676–10681.
41. Chen JM, et al. (2012) EspD is critical for the virulence-mediating ESX-1 secretion system in *Mycobacterium tuberculosis*. *J Bacteriol* 194(4):884–893.
42. Tan S, Sukumar N, Abramovitch RB, Parish T, Russell DG (2013) *Mycobacterium tuberculosis* responds to chloride and pH as synergistic cues to the immune status of its host cell. *PLoS Pathog* 9(4):e1003282.
43. Marrakchi H, Lanéelle G, Quémard A (2000) InhA, a target of the antituberculous drug isoniazid, is involved in a mycobacterial fatty acid elongation system, FAS-II. *Microbiology* 146(Pt 2):289–296.
44. Bruning JB, Murillo AC, Chacon O, Barletta RG, Sacchettini JC (2011) Structure of the *Mycobacterium tuberculosis* D-alanine:D-alanine ligase, a target of the antituberculosis drug D-cycloserine. *Antimicrob Agents Chemother* 55(1):291–301.
45. Solapure S, et al. (2013) In vitro and in vivo efficacy of β-lactams against replicating and slowly growing/nonreplicating Mycobacterium tuberculosis. *Antimicrob Agents Chemother* 57(6):2506–2510.
46. Sani M, et al. (2010) Direct visualization by cryo-EM of the mycobacterial capsular layer: A labile structure containing ESX-1-secreted proteins. *PLoS Pathog* 6(3):e1000794.
47. Kelley LA, Sternberg MJ (2009) Protein structure prediction on the Web: A case study using the Phyre server. *Nat Protoc* 4(3):363–371.
48. Parida BK, Douglas T, Nino C, Dhandayuthapani S (2005) Interactions of anti-sigma factor antagonists of *Mycobacterium tuberculosis* in the yeast two-hybrid system. *Tuberculosis (Edinb)* 85(5-6):347–355.
49. Geiman DE, et al. (2004) Attenuation of late-stage disease in mice infected by the *Mycobacterium tuberculosis* mutant lacking the SigF alternate sigma factor and identification of SigF-dependent genes by microarray analysis. *Infect Immun* 72(3): 1733–1745.
50. Williams EP, Lee JH, Bishai WR, Colantuoni C, Karakousis PC (2007) *Mycobacterium tuberculosis* SigF regulates genes encoding cell wall-associated proteins and directly regulates the transcriptional regulatory gene *phoY1*. *J Bacteriol* 189(11):4234–4242.
51. Dhandayuthapani S (2007) Stress response of genes encoding putative stress signaling molecules of *Mycobacterium tuberculosis*. *Front Biosci* 12:4676–4681.
52. Hartkoorn RC, et al. (2012) Genome-wide definition of the SigF regulon in *Mycobacterium tuberculosis*. *J Bacteriol* 194(8):2001–2009.
53. Duncan L, Alper S, Losick R (1996) SpoIIAA governs the release of the cell-type specific transcription factor sigma F from its anti-sigma factor SpoIIAB. *J Mol Biol* 260(2): 147–164.
54. Garces A, et al. (2010) EspA acts as a critical mediator of ESX1-dependent virulence in *Mycobacterium tuberculosis* by affecting bacterial cell wall integrity. *PLoS Pathog* 6(6):e1000957.
55. Raghavan S, Manzanillo P, Chan K, Dovey C, Cox JS (2008) Secreted transcription factor controls *Mycobacterium tuberculosis* virulence. *Nature* 454(7205):717–721.
56. Abdallah AM, et al. (2007) Type VII secretion—mycobacteria show the way. *Nat Rev Microbiol* 5(11):883–891.
57. Mizuno T, Mizushima S (1990) Signal transduction and gene regulation through the phosphorylation of two regulatory components: The molecular basis for the osmotic regulation of the porin genes. *Mol Microbiol* 4(7):1077–1082.
58. Heermann R, Jung K (2010) The complexity of the 'simple' two-component system KdpD/KdpE in *Escherichia coli*. *FEMS Microbiol Lett* 304(2):97–106.
59. Steyn AJ, Joseph J, Bloom BR (2003) Interaction of the sensor module of *Mycobacterium tuberculosis* H37Rv KdpD with members of the Lpr family. *Mol Microbiol* 47(4): 1075–1089.
60. Möker N, et al. (2004) Deletion of the genes encoding the MtrA-MtrB two-component system of *Corynebacterium glutamicum* has a strong influence on cell morphology, antibiotics susceptibility and expression of genes involved in osmoprotection. *Mol Microbiol* 54(2):420–438.
61. Ho TD, Ellermeier CD (2012) Extra cytoplasmic function σ factor activation. *Curr Opin Microbiol* 15(2):182–188.
62. Greenstein AE, Echols N, Lombana TN, King DS, Alber T (2007) Allosteric activation by dimerization of the PknD receptor Ser/Thr protein kinase from *Mycobacterium tuberculosis*. *J Biol Chem* 282(15):11427–11435.
63. Good MC, Greenstein AE, Young TA, Ng HL, Alber T (2004) Sensor domain of the *Mycobacterium tuberculosis* receptor Ser/Thr protein kinase, PknD, forms a highly symmetric beta propeller. *J Mol Biol* 339(2):459–469.
64. Baer CE (2010) Mechanisms of *Mycobacterium tuberculosis* serine/threonine protein kinase activation. PhD dissertation (Univ of California, Berkeley, CA).
65. Kovacs H, Comfort D, Lord M, Campbell ID, Yudkin MD (1998) Solution structure of SpoIIAA, a phosphorylatable component of the system that regulates transcription factor sigmaF of *Bacillus subtilis*. *Proc Natl Acad Sci USA* 95(9):5067–5071.
66. Barik S, Sureka K, Mukherjee P, Basu J, Kundu M (2010) RseA, the SigE specific anti-sigma factor of *Mycobacterium tuberculosis*, is inactivated by phosphorylation-dependent ClpC1P2 proteolysis. *Mol Microbiol* 75(3):592–606.
67. Mehra S, Kaushal D (2009) Functional genomics reveals extended roles of the *Mycobacterium tuberculosis* stress response factor sigmaH. *J Bacteriol* 191(12):3965–3980.
68. Sherrid AM, Rustad TR, Cangelosi GA, Sherman DR (2010) Characterization of a Clp protease gene regulator and the reaeration response in *Mycobacterium tuberculosis*. *PLoS One* 5(7):e11622.
69. Eymann C, et al. (2011) In vivo phosphorylation patterns of key stressosome proteins define a second feedback loop that limits activation of *Bacillus subtilis* sigmaB. *Mol Microbiol* 80(3):798–810.
70. Marles-Wright J, et al. (2008) Molecular architecture of the "stressosome," a signal integration and transduction hub. *Science* 322(5898):92–96.
71. Beaucher J, et al. (2002) Novel *Mycobacterium tuberculosis* anti-sigma factor antagonists control sigmaF activity by distinct mechanisms. *Mol Microbiol* 45(6):1527–1540.
72. Malik SS, Luthra A, Ramachandran R (2009) Interactions of the *M. tuberculosis* UsfX with the cognate sigma factor SigF and the anti-anti sigma factor RsfA. *Biochim Biophys Acta* 1794(3):541–553.
73. Bugrysheva J, Froehlich BJ, Freiberg JA, Scott JR (2011) Serine/threonine protein kinase Stk is required for virulence, stress response, and penicillin tolerance in *Streptococcus pyogenes*. *Infect Immun* 79(10):4201–4209.
74. Lamichhane G, et al. (2003) A postgenomic method for predicting essential genes at subsaturation levels of mutagenesis: Application to *Mycobacterium tuberculosis*. *Proc Natl Acad Sci USA* 100(12):7213–7218.
75. Rustad TR, Harrell MI, Liao R, Sherman DR (2008) The enduring hypoxic response of *Mycobacterium tuberculosis*. *PLoS One* 3(1):e1502.
76. Hugonnet JE, Tremblay LW, Boshoff HI, Barry CE, 3rd, Blanchard JS (2009) Meropenem-clavulanate is effective against extensively drug-resistant *Mycobacterium tuberculosis*. *Science* 323(5918):1215–1218.
77. Peters PJ, Bos E, Griekspoor A (2006) Cryo-immunogold electron microscopy. *Curr Protoc Cell Biol* Chap 4, Unit 4.7.
78. Pease DC (1964) *Histological Techniques for Electron Microscopy* (Academic, New York).
79. Stenberg PE, Shuman MA, Levine SP, Bainton DF (1984) Redistribution of alpha-granules and their contents in thrombin-stimulated platelets. *J Cell Biol* 98(2): 748–760.